(100) orientation-controlled Ge giant-stripes on insulating substrates by rapid-melting growth combined with Si micro-seed technique

Toko, Kaoru
Department of Electronics, Kyushu University

Kurosawa, Masashi
Department of Electronics, Kyushu University

Yokoyama, Hiroyuki
Department of Electronics, Kyushu University

Kawabata, Naoyuki
Department of Electronics, Kyushu University

他

出版情報：Applied Physics Express. 3 (7), pp.075603(1)-075603(3), 2010-07. 応用物理学会
バージョン：

(100) Orientation-Controlled Ge Giant-Stripes on Insulating Substrates by Rapid-Melting Growth Combined with Si Micro-Seed Technique

Kaoru TOKO*, Masashi KUROSAWA, Hiroyuki YOKOYAMA, Naoyuki KAWABATA, Takashi SAKANE, Yasuharu OHTA, Takanori TANAKA, Taizoh SADOH, and Masanobu MIYAO[+]

Department of Electronics, Kyushu University, 744 Motooka, Fukuoka, 819-0395, Japan

Orientation-controlled single-crystal Ge stripes on insulating substrates are desired to achieve high-performance thin-film transistors. The rapid-melting growth process of amorphous Ge has been examined by using polycrystalline Si islands as the growth seed. Rotational growth is found for Ge stripes initiated from (110) and (111) orientations, however, the lateral-growth initiated from the (100) orientation propagates continuously keeping its orientation. Based on these findings, an advanced rapid-melting growth method is developed by combining with the Si (100) micro-seed technique. This enables single-crystal Ge (100) giant-stripes with 400 μm length on insulating substrates. High hole mobility exceeding 1000 cm^2/Vs is also demonstrated.

* k_toko@nano.ed.kyushu-u.ac.jp

[+] miyao@ed.kyushu-u.ac.jp

High carrier mobility in the single-crystalline Ge is very attractive for thin-film transistors (TFTs) with ultra-high speed operation.[1,2] Since channel mobility and threshold voltage in TFTs depend on crystal orientation,[3] single crystalline Ge areas with identical orientation should be formed on the transparent insulating substrates. To achieve high-performance system-in-displays, many researchers have developed advanced crystal growth techniques enabling high-quality Ge films on insulating substrates.[4-10] However, single-crystalline Ge films with controlled-orientation have not been realized on insulating substrates.

Recently, the seeding rapid-melting-growth of amorphous-Ge (a-Ge) films has been examined on SiO_2 or Si_3N_4 islands deposited on Si substrates, where crystalline Si (Si substrate) was employed as crystal seed to initiate rapid-melting-growth.[11-15] We investigated the detail of this process, and clarified that the driving force to cause lateral growth is not the thermal flow from the molten-Ge to the Si substrates through seeding windows, but the spatial gradient of the solidification temperature originating from Si-Ge mixing at seeding areas.[14,16] On the basis of this finding, we developed the Si-substrate-free rapid-melting-growth of a-Ge by employing the polycrystalline Si (poly-Si) islands as growth seeds.[17,18] This realized giant single-crystal Ge stripes with 400 μm length (width: 3 μm) on quartz substrates, which demonstrated very high carrier mobility (1040 cm^2/Vs).[17] However, crystal orientations of the Ge stripes were distributed into (100), (110), and (111) directions reflecting the orientation of the poly-Si grains. Such random distributions of the crystal-orientations should be controlled to achieve high-performance TFT arrays.

In this work, the Ge-growth features of the Si-substrate-free rapid-melting process are clarified by investigating their distributed crystal orientation statistically. Based on this knowledge, rapid-melting-growth is combined with the Si (100) micro-seed technique, recently developed by our group.[19] This achieves (100) orientation-controlled

single-crystalline Ge (100) stripes on quartz substrates.

In the experiments, a-Si (100 nm thickness) were deposited on insulating substrates, i.e., quartz substrates and Si_3N_4 films (100 nm thickness) formed on Si substrates, by using a molecular beam epitaxy (MBE) system (base pressure: 5×10^{-10} Torr). After poly-crystallization by furnace annealing (650^{o}C, 15 h), they were patterned by wet etching to form island areas, which were used as the seed for lateral growth. Subsequently, a-Ge layers (100 nm thickness) were deposited using the MBE system, and they were patterned into narrow stripe lines (400 μm length, 5 μm width), as shown in Fig. 1(a). Then SiO_2 films (800 nm thickness) were deposited by RF magnetron sputtering. Finally, these samples were heat-treated by rapid thermal annealing (RTA) at 1000^{o}C (1 s) to induce the rapid-melting growth from the seeding areas. The morphology, crystal orientation, and crystal quality of the grown layers were characterized by Nomarski optical microscopy, electron backscattering diffraction (EBSD), and micro-probe Raman spectroscopy (spot size: ~1 μmϕ), respectively. In addition, carrier mobility was evaluated by measuring the temperature dependence of the electrical conductivity.

A typical Nomarski optical micrograph of the annealed sample (substrate: Si_3N_4/Si) is shown in Fig. 1(b), which indicates the formation of a uniform and flat Ge stripe with 400 μm length. Such a uniform morphology was also obtained for samples formed on quartz substrates.[17] Two typical EBSD images obtained from many samples are shown in Figs. 1(c) and 1(d), which display the orientation-mapping of the sample surfaces (Z plane). The image shown in Fig. 1(c) indicates the Ge growth with a constant orientation [(100) plane] in the whole length (400 μm), where no grain boundaries were observed. This indicates that single-crystal Ge growth is obtained, even though poly-Si islands with random orientations [insert of Fig. 1(a)] are used for the growth seed. Such an orientation-selecting process from multi-grains (poly-Si seed) will be discussed later. On

the other hand, Fig. 1(d) obtained from another sample shows the gradual change of their orientations [from (111) to (100) plane] along the growth direction.

The crystal orientation parallel to the growth direction (X plane) was also measured. Interestingly, it was found that the orientation in X plane was kept constant (<101> direction) throughout the growth for all samples. Data obtained from the sample shown in Fig. 1(d) is shown in Fig. 1(e). These orientation-mappings in Z and X planes [Figs. 1(d) and 1(e)] suggest that crystal growth initiated from the (111) plane propagates laterally with rotating its crystal orientation. Similar results were also obtained for samples using quartz substrates.[17)]

The rotating growth phenomena are quantitatively examined as a function of the distance from the poly-Si seed by analyzing the EBSD data. In Fig. 2(a), the crystal orientations of Ge surfaces are summarized as the angular difference from the (100) plane. Here, results for the Ge stripe initiated from the (111) orientation [sample shown in Fig. 1(d)] are shown by open circles. It is clear that crystal orientation gradually rotates from (111) plane and abruptly stabilizes when the orientation reaches the (100) plane (about 200 μm away from the Si-seed). Results for the Ge stripe initiated from the (100) orientation [sample shown in Fig. 1(c)] are also shown by solid circles, which show the stabilized lateral growth keeping its orientation.

The full widths at half maximum (FWHM) of the Ge-Ge peaks locating at 300 cm^{-1} in the Raman spectra are summarized in Fig. 2(b). The small FWHM value of 3.3 cm^{-1} is obtained in the whole growth-region for the rotation-free samples [the sample shown in Fig. 1(c)]. These values were almost the same with that measured for a single-crystal Ge-bulk (3.2 cm^{-1}), and smaller than those (5.0–8.3 cm^{-1}) reported for samples obtained by solid phase crystallization[4,5)] and laser annealing methods [7,8)] These results indicate the high crystal quality of our rotation-free Ge stripes. For the rotationally grown Ge stripe [the sample shown in Fig. 1(d)], large FWHM values (~ 3.8 cm^{-1}) are obtained in the

intermediate region (30-200 μm from the Si-seed) along the growth, where crystal rotation from (111) to (100) orientations is visible [see Fig. 2(a)]. Additional experiments using bulk-Ge wafers with different orientations [(100), (101), (111)] indicated that the FWHM value did not depend on the crystal orientations. Consequently, results shown in Figs. 2(a) and 2(b) suggest the introduction of defects in the rotationally growth region. In other words, suppression of the rotational growth is essential to apply such Ge-stripes for the high-performance devices.

To solve two crucial questions, i.e., what determines the initial crystal orientation of Ge starting from ploy-Si seed, and what causes the crystal rotation during the lateral growth, we examined the rapid-melting growth phenomenon statistically. The fractions of crystal orientations (Z plane) in poly-Si grains, Ge grown-layers near (~10 μm) the seeding edges and Ge at the growth edge (~350 μm away from the seed) are shown in Figs. 3(a)-3(c), respectively. Dynamical-change in crystal orientations in each Ge stripe during lateral growth is also examined for many samples. They are summarized in Fig. 3(d) as a function of the distance from the Si-seed. In these figures, the crystal orientations within 15^{o} from the exact (100), (101), and (111) orientations are classified into (100), (101), and (111) groups. In addition, the data obtained for the samples using Si_3N_4/Si and quartz substrates are shown by the blue and red bars [Figs. 3(a)-3(c)] or lines [Fig. 3(d)], respectively.

These results show that the orientation distributions of Ge layers near the Si-seed [Fig. 3(b)] quite agree with those of poly-Si islands [Fig. 3(a)] for both samples with Si_3N_4/Si and quartz substrates. This indicates that one of the crystal-grains in the poly-Si island incidentally acts as the seed to cause the rapid-melting growth of the Ge stripes.

On the other hand, the orientation distributions of Ge at the growth edge [Fig. 3(c)] show that as many as 70% of Ge layers are oriented to the (100) plane and the rest to the (101) plane. Results shown in Fig. 3(d) clearly indicate that the randomly distributed

crystal-orientations in the initial stage gradually converge to the (100) plane through (101) plane. In 1980's, micro-zone melting growth of Ge has been intensively examined, which demonstrated that (100) oriented growth was preferentially propagated on SiO_2 substrates due to the lowest interfacial free energy between (100) Ge and SiO_2 layers.[9,10] These results well explain the present results, where (100) oriented growth becomes dominant at the final stage of the rapid-melting growth.

The fact that all Ge initiated with the (100) plane grows continuously with keeping its orientation, is particularly worth noting. This triggers the idea of advanced rapid-melting growth method combined with the (100) Si micro-seed technique. Very recently, we have developed the interfacial-oxide modulated aluminum-induced crystallization (AIC) method, which achieved the formation of (100) Si crystal-grains on quartz substrates.[19] Such (100) Si crystal-grains are the candidate to be used as seed for the rapid-melting Ge growth.

The sample structure is schematically shown in Fig. 4. The insertion (Fig. 4(a)) shows the EBSD image of the Si island (100 nm thickness) formed by the interfacial-oxide modulated AIC method, which indicates the Si crystal grains preferentially (90%) orientated to the (100) plane. The grain size (~30 μmϕ) is large enough to be employed as single-crystal Si seeds for the growth of narrow Ge stripes (5 μm width).

After rapid thermal annealing (1000^{o}C, 1 s), electron diffraction patterns of the Si island (seed), the Ge region vertically grown from the Si seed, and the laterally grown Ge region 300 μm away from the Si seed were measured. They are displayed in Figs. 4(b)-4(d), which clearly show the Kikuchi patterns. Detailed analysis confirms that the orientation of the Ge region completely agrees with that of the single crystalline Si seed. EBSD images of the Ge stripes analyzed from two perpendicular directions (Z and X planes) are displayed in Fig. 4(e), which exhibits the (100)-oriented single crystal Ge

growth in the whole region. These results demonstrate that the epitaxial growth of a-Ge is initiated from the (100) Si micro-seed and propagates 400 μm with keeping its orientation.

Crystal structures of the grown layers are also characterized by cross-sectional transmission electron microscopy (TEM), which clearly indicates the high crystal quality without dislocations or stacking faults. The electrical characteristics of Ge stripes are also evaluated for many samples by measuring the temperature dependence of the electrical conductivity. This demonstrated the high hole mobility of 1150±50 cm^2/Vs for all samples. Very sharp dispersion of the mobility distribution (1150±50 cm^2/Vs) indicates that the orientation-controlled rapid melting growth enables the uniform-formation of single-crystalline Ge stripe arrays on insulating substrates.

In summary, crystal orientations of Ge stripes obtained by the Si-substrate-free rapid-melting-growth method, where poly-Si islands are used as growth seeds, have been examined comprehensively. Statistical studies have clarified that the Ge growth starting with (100) orientation is the key points to achieve the orientation-controlled Ge lateral-growth on insulating substrates. This has triggered the development of the advanced rapid-melting growth method combining with the Si (100) micro-seed technique. As a result, single-crystal (100) Ge giant-stripes with 400 μm length have been achieved on insulating substrates, which demonstrate high hole mobility exceeding 1000 cm^2/Vs. This orientation-controlled rapid-melting growth method opens up the possibility of Ge-based TFTs with high speed operation.

Acknowledgements

A part of this work was supported by Semiconductor Technology Academic Research Center (STARC) and a Grant-in-Aid for Scientific Research from the Ministry of Education, Culture, Sports, Science, and Technology, Japan. Valuable comments by Drs. I. Mizushima, N. Tamura, and M. Yoshimaru of STARC are greatly appreciated.

References

1) M. Miyao, E. Murakami, H. Etoh, K. Nakagawa, and A. Nishida: J. Cryst. Growth **111** (1991) 912.

2) G. Taradchi, A. J. Pitera, and E. A. Fitzgerald: Solid-State Electron. **48** (2004) 1297.

3) C. H. Lee, T. Nishimura, N. Saido, K. Nagashio, K. Kita, A. Toriumi: IEDM Tech. Dig., (2009) 19.2.

4) Y. C. Tsao, W. J. Weber, P. Campbell, I. P. Widenborg, D. Song, and A. M. Green: Appl. Surf. Sci. **255** (2009) 7028.

5) K. Toko, I. Nakao, T. Sadoh, T. Noguchi, and M. Miyao: Solid-State Electron. **53** (2009) 1159.

6) H. Watakabe, T. Sameshima, H. Kanno, T. Sadoh, and M. Miyao: J. Appl. Phys. **95** (2004) 6457.

7) W. Yeh, H. Chen, H. Huang, C. Hsiao, and J. Jeng: Appl. Phys. Lett. **93** (2008) 094103.

8) K. Sakaike, S. Higashi, H. Murakami, and S. Miyazaki: Thin Solid Films **516** (2008) 3595.

9) M. Takai, T. Tanigawa, M. Miyauchi, S. Nakashima, K. Gamo, and S. Namba: Jpn. J. Appl. Phys. **23** (1984) L363.

10) K. Sakano, K. Moriwaki, H. Aritome, and S. Namba: Jpn. J. Appl. Phys. **21** (1982) L636.

11) Y. Liu, M. D. Deal, and D. Plummer: Appl. Phys. Lett. **84** (2004) 2563.

12) D. J. Tweet, J. J. Lee, J. S. Maa, and S. T. Hsu: Appl. Phys. Lett. **87** (2005) 141908.

13) F. Gao, S. J. Lee, S. Balakumar, A. Du, Y. L. Foo, and D. L. Kwong: Thin Solid Films **504** (2006) 69.

14) M. Miyao, T. Tanaka, K. Toko, and M. Tanaka: Appl. Phys. Express **2** (2009)

045503.

15) T. Hashimoto, C. Yoshimoto, T. Hosoi, T. Shimura, and H. Watanabe: Appl. Phys. Express **2** (2009) 066502.

16) T. Tanaka, K. Toko, T. Sadoh, and M. Miyao: Appl. Phys. Express **3** (2010) 031301.

17) M. Miyao, K. Toko, T. Tanaka, and T. Sadoh: Appl. Phys. Lett. **95** (2009) 022115.

18) K. Toko, T. Sakane, T. Tanaka, T. Sadoh, and M. Miyao: Appl. Phys. Lett. **95** (2009) 112107.

19) M. Kurosawa, N. Kawabata, T. Sadoh, and M. Miyao: Appl. Phys. Lett. **95** (2009) 132103.

Figure Captions

Fig. 1 Schematic sample structure (a), Nomarski optical micrograph of a Ge stripe on a Si_3N_4 film after RTA (1000^oC, 1 s) (b), EBSD images of Ge stripes on Si_3N_4 without (c) and with rotational growth (d), (e), where [z] and [x] show the observed directions of the crystal orientations. The insertion in (a) shows an EBSD image of a poly-Si seed on a Si_3N_4 film.

Fig. 2 Angular difference from (100) plane (a) and FWHM of Raman peaks due to Ge-Ge vibration mode (b) as a function of distance from Si-seed, where the solid and open circles show the data of the samples shown in Figs. 1(c) and 1(d), respectively.

Fig. 3 Distribution of crystal orientations in poly-Si seed (a), Ge layers near the seed (b) and at the growth edge (c), and transition-chart of crystal orientations for each Ge stripes (27 samples) as a function of distance from Si-seed (d). Here the results for samples with Si_3N_4 and quartz substrates are shown by blue and red, respectively.

Fig. 4 EBSD images in [z] plane of the AIC-Si island (a), ED patterns (Kikuchi patterns) on the AIC-Si (100) seed (b), vertically grown Ge on the Si seed (c), and laterally grown Ge (d), and EBSD images in [z] and [x] planes of the rapid-melt grown Ge stripe on a quartz substrate (e).

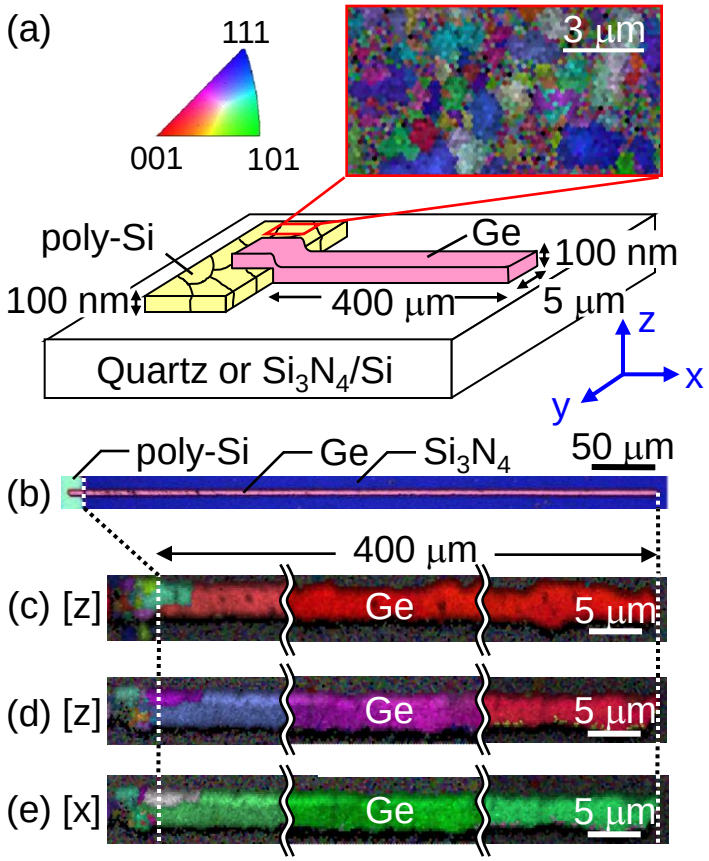

Figure 1: K. Toko

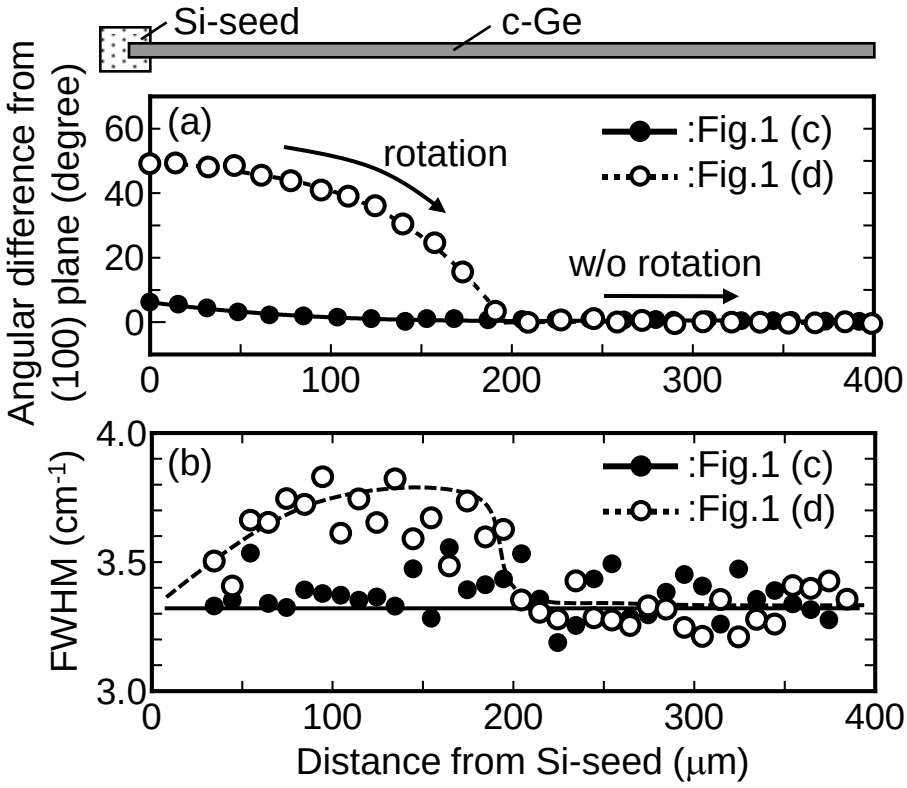

Figure 2: K. Toko

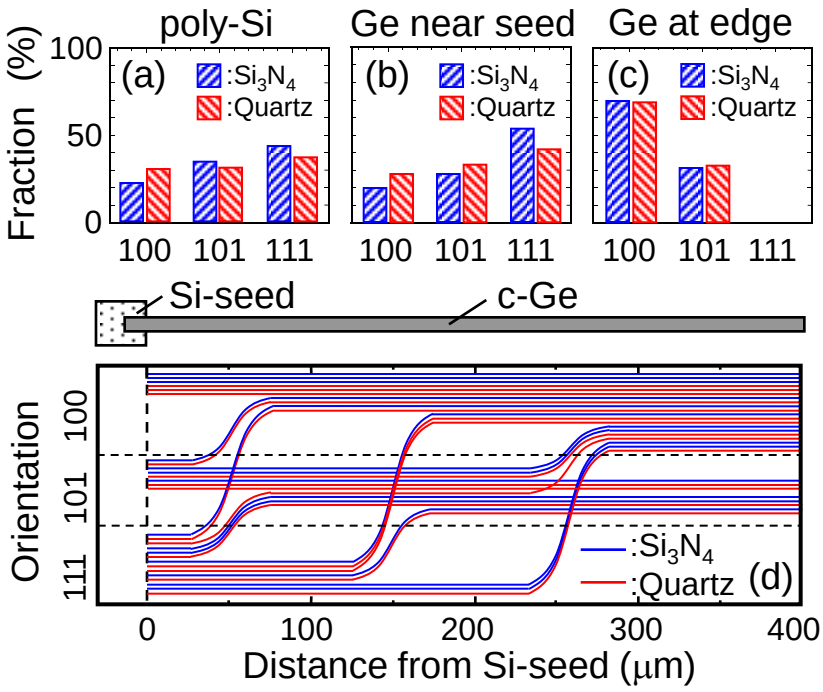

Figure 3: K. Toko

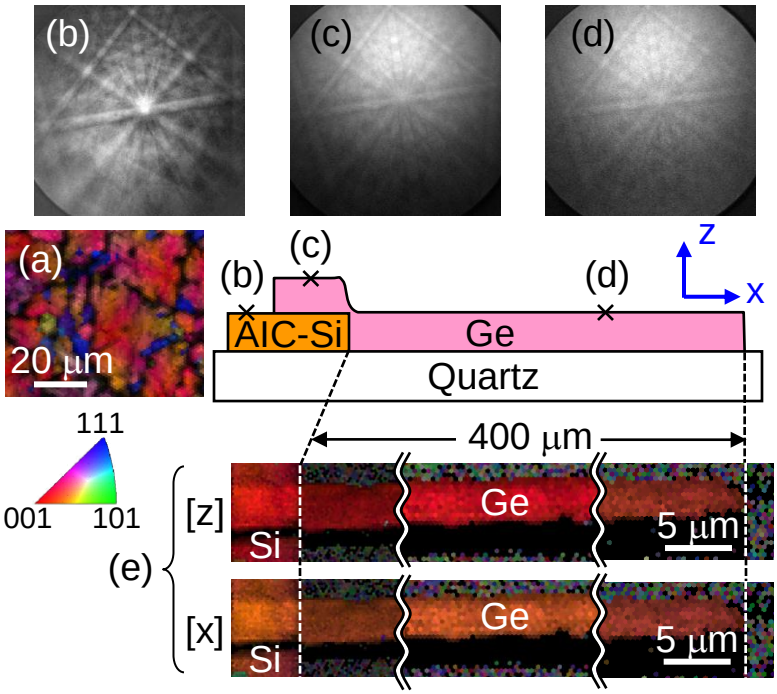

Figure 4: K. Toko